NOTICE

CERTAIN DATA CONTAINED IN THIS DOCUMENT MAY BE DIFFICULT TO READ IN MICROFICHE PRODUCTS.

Conf-920430--85

PNL-SA--20408

DE92 012338

CORROSION RESISTANCE OF STAINLESS STEELS AND HIGH NI-CR ALLOYS TO ACID FLUORIDE WASTES

H. D. Smith
D. B. Mackey
K. H. Pool
E. B. Schwenk

April 1992

Presented at the
American Nuclear Society International High Level Radioactive Waste Management
April 12-16, 1992
Las Vegas, Nevada

Work supported by
the U.S. Department of Energy
under Contract DE-AC06-76RLO 1830

Pacific Northwest Laboratory
Richland, Washington 99352

CORRODION RESISTANCE OF STAINLESS STEELS AND HIGH NI-CR ALLOYS TO ACID FLUORIDE WASTES

F. L. Smith
Pacific Northwest Laboratory
P.O. Box 999
Richland, WA 99352
(509)376-3588

J. L. Ross
Pacific Northwest Laboratory
P.O. Box 999
Richland, WA 99352
(509)376-1753

D. B. Mackey
Pacific Northwest Laboratory
P.O. Box 999
Richland, WA 99352
(509)376-9844

E. B. Schwenk
Westinghouse Hanford Company
P.O. Box 1970
Richland, Wa 99352
(509)376-4917

ABSTRACT

TRUEX processing of Hanford Site waste will utilize potentially corrosive acid fluoride processing solutions. Appropriate construction materials for such a processing facility need to be identified. Toward this objective, candidate stainless steels and high Ni-Cr alloys have been corrosion tested in simulated acid fluoride process solutions at 333K. The high Ni-Cr alloys exhibited corrosion rates as low as 0.14 mm/y in a solution with an HF activity of about 1.2 M, much lower than the 19 to 94 mm/y observed for austenitic stainless steels. At a lower HF activity (about 0.008 M), stainless steels display delayed passivation while high Ni-Cr alloys display essentially no reaction.

I. INTRODUCTION

The Transuranic Extraction (TRUEX) process will be used at the Hanford Site to separate transuranic (TRU) elements from radioactive liquid/slurry wastes to produce two waste streams. It is anticipated that the small-volume TRU stream will eventually be processed into glass at the Hanford Waste Vitrification Plant (HWVP), and the large-volume, non-TRU stream will be immobilized as grout.

There are three principal types of liquid/slurry waste, also called double-shell tank (DST) waste, to be processed: neutralized cladding removal waste (NCRW), complexant concentrate waste (CC), and plutonium finishing plant waste (PFP). Waste processing includes dilution and transfer of the waste to the TRUEX facility where it will be acidified to 1 to 2 M hydrogen ion concentration (H^+) before the transuranic elements are removed.

The contents of the individual DSTs are stratified and include a variety of compositions, some of which are high in fluoride (up to 3 to 8 M). Table 1 shows the variation of the observed NCRW waste composition in a typical tank. Depending on the relative amounts of fluoride and fluoride complexing agents, such as boron, aluminum, and zirconium, these compositions may produce very corrosive solutions when acidified.[1]

Because some of the potential solutions are highly corrosive, Westinghouse Hanford Company has initiated corrosion studies of candidate TRUEX processing plant alloys at Pacific Northwest Laboratory[a] for the U.S. Department of Energy (DOE). The immediate objective of the investigation is the reduction of the number of candidate plant alloys, using uniform corrosion under expected TRUEX chemical processing conditions as the criterion of worth. The simulated process solutions used as the corrosion test environments (Table 2) cover the upper range of hydrofluoric acid activities expected for the TRUEX processing solutions. They (A and B Table 2) were chosen to represent an extreme and an intermediate condition of expected corrosivity. The results of these initial tests will allow us to focus on specific alloys in later, more comprehensive testing.

---

[a]Pacific Northwest Laboratory is operated by Battelle Memorial Institute for the U.S. Department of Energy under Contract DE-AC06-76RLO-1830.

TABLE 1. Concentration (M) Range for Nonradioactive Species in Neutralized Cladding Removal Waste from Tank 103-AW

Specie	Concentration Maximum	Concentration Minimum
Na	15.9	1.08
Al	2.35	0.0016
Zr	1.79	0.0013
Cr	0.38	1.8×10^{-5}
K	0.59	0.056
B	0.12	2.8×10^{-4}
Ni	0.47	0.011
Ca	0.018	2.3×10^{-4}
Fe	0.021	1.8×10^{-5}
Mn	9.8×10^{-3}	8.8×10^{-5}
F	6.2	0.002
Cl	0.18	0.004
CO_3	0.26	0.02
NH_4	0.021	0.005
NO_2	1.48	0.017
NO_3	0.14	0.043
OH	1.95	0.57
SO_4	0.014	0.000

TABLE 2. Compositions of TRUEX Process Solution Simulants

A) 2 M HNO_3
2 M NaF
HF ~1.2 M

B) 0.95 M F^- as NaF
0.275 M Zr^{+4} as $ZrO(NO_3)_2 \cdot 2H_2O$
0.045 M Si^{+4} as $Na_2SiO_3 \cdot 9H_2O$
0.01 M B^{+3} as H_3BO_3
0.263 M Cl^- as NaCl
HNO_3 to obtain 1.5 M H^+
HF ~0.008 M

II BACKGROUND

HF-HNO_3 solutions are corrosive to all non-noble metal alloy systems. The high Ni-Cr alloys (e.g., certain Hastelloys[a] and Inconels[b]) show relatively low corrosion rates at low HF concentrations (<1.0 M HF) in these solutions. The corrosion rate increases with HF concentration, e.g. a 1% HF addition to a 20% nitric acid solution increases the corrosion rate of the Hastelloys at 353K (80°C) from 1 to 10 mpy to 30 to 400 mpy. Further additions result in smaller increases[2]. Ondrejcin and McLaughlin (1980)[3] studied a series of 304L and high Ni-Cr alloys (increasing in Ni+Cr content from 304L to Inconel 671) in 0.01 M HF + 10 M HNO_3 and 0.10 M HF + 10 M HNO_3 solutions at temperatures up to 403K (130°C). They measured a minimum corrosion rate of about 25 mpy at 373K in 0.01 M HF to 10 M HNO_3 solutions, and concluded that the HF concentration must remain below 0.01 M for the alloys studied to be useful in solutions similar to TRUEX test solutions.

A number of investigators including Maness (1959,[4] 1964)[5] Newby and Hoffman (1967,[6] these have been summarized by Cole 1974),[7] and more recently Ondrejcin and McLaughlin (1980), have shown that the presence of metal ions such as aluminum and zirconium in the acid fluoride solutions substantially reduces the corrosivity of the solutions. The reduction in corrosivity was observed for 304L and a series of higher Ni-Cr alloys because these metal ions (i.e., Al^{+3}, Zr^{+4}) more strongly complex the fluoride than do the alloy components and reduce the HF activity in the solutions. This is consistent with the work of Hammer (1979),[8] who determined the degree to which fluoride complexes elements such as zirconium and aluminum in acid fluoride solution at concentrations and temperatures similar to those employed in this study. A simplified relationship based on Hammer's work is given in equation [1].

$$F_t (1 - N_{av}/R) = [HF/HNO_3] \times [HNO_3] \quad [1]$$

where F_t is the total fluoride concentration,

N_{av} is the average number of fluoride ions complexed to the metal ion, and

R is the ratio of total fluoride ion to total complexing metal ion.

Solution B, with a nominal F/Zr ratio (R) of 0.95/0.275 = 3.45 and N_{av} about 3.42, has an HF activity of about 0.008 M_{HF}. The HF activity of solution A is about 1.2 M_{HF}. Hence, the activity of HF in solution A is about 160 times the activity of HF in solution B. If HF is the principal corrosion agent in these solutions, then solution A should be much more corrosive than solution B.

III DESCRIPTION OF CORROSION STUDY

The present corrosion study was carried out using Teflon[c] jars with a capacity of 0.002 m^3 (2000 mL) placed in a 333K water bath. Teflon condensers extended above the screw-on lids. The condensers allowed venting of the jars to the atmosphere while preventing significant water loss. At least 1.25×10^{-4} m^3 (125 mL) of solution per 6.45 cm^2 (square inch) of submerged metal coupon was

[a] Hastelloy is a trademark of Haynes International Company, Kokomo, Indiana.
[b] Inconel is a trademark of the International Nickel Company, New York, New York.
[c] Teflon is a registered trademark of Dupont de Nemours, Inc., Wilmington, Delaware.

placed in each jar. Nine coupons were hung on a Teflon specimen rack in the jars (3 completely submerged, 3 half submerged, and 3 hung in the vapor phase). This three-environment test covers the range of service conditions to which a material might be exposed as a component of a chemical processing system.

Rectangular corrosion coupons with nominal dimensions of 3.81 cm x 1.27 cm x 0.159 cm, with a 0.64 cm hole at one end, were used for these experiments. Each coupon was carefully weighed (to 10^{-4} g) and measured (to 2.5×10^{-3} cm) prior to corrosion exposure. Following each exposure period, the coupons were carefully rinsed in deionized water, ethanol, and oil-free acetone, in that order. During the rinsing, each coupon surface was brushed with a soft bristle brush to remove weakly adhering corrosion scale. The removal of the scale was completed using a wooden implement, but care was taken not to forcefully abrade the metal surface. Average uniform corrosion rates were computed from the measured time in the corrosion environment, the measured weight change, and the initial coupon surface area. Corrosion rates were not calculated from the weight change of coupons that had significant corrosion scale adhering to them that could not be easily removed, as described above.

Eighteen candidate alloys were chosen to cover the range of available Ni-Cr alloys from 304L (26% Cr+Ni) to Inconel 671 (99.4% Cr+Ni). All coupons had a standard 120-grit sanded finish and were fabricated from stock having certified compositions (Table 3).

IV. RESULTS

A. Corrosion Rates

In general, it was observed that the vapor phase corrosion was negligible except for very susceptible materials such as austenitic stainless steels over solution A. The higher Ni-Cr alloys displayed little reaction in the vapor phase above the solution, except for significant intergranular corrosion on Inconel 617 and some endgrain pitting on the other alloys, all above solution A. Also, no significant attack was observed associated with the liquid interface. This report therefore concentrates only on results from the fully submerged coupons.

Corrosion rates in solution A at 333K decreased logarithmically as the Cr+Mo content of the alloy increased. The decrease of the corrosion rate was quite dramatic as the Cr+Mo content increased from about 18% to 25%. The measured corrosion rate continued to decrease with increasing Cr+Mo beyond 25%, but with a significantly weaker dependence. These results are summarized in Figure 1. There appear to be two trends, as suggested by the solid lines in the figure. The alloys following the trend having the higher corrosion rate generally a) do not contain minor alloying elements such as copper and tungsten, or b) are low in chromium. Only Hastelloy 276 and Hastelloy C-4 do not fit this alloy composition pattern.

During the tests a sodium metal fluoride scale (described in more detail in the next section) tended to form on the coupons and adhere with varying degrees of tenacity. The data included in Figure 1 were taken at a point in the test where the scale influence was believed still minimal (i.e., incomplete coverage and nonadherent). In some cases described later in this section, the coupons of some alloys were virtually passivated by the scale. Table 4 lists the alloys plotted in Figure 1 and the length of time the coupons were exposed to solution A before the corrosion rate was determined. Interference of the scale in accurately determining weight change occurred early in testing for some alloys and much later for others. The stainless steel tests were run for only a short time because of rapid corrosion in solution A.

Initially, Inconel 671 showed about the same uniform corrosion rate as C-22 and G-30 in solution A at 333K, but specimens of this alloy and the other Inconels (except Inconel 625) soon developed an adherent corrosion scale. A metallographic examination showed that Inconel 671, 617, and 690 were undergoing intergranular corrosion but to different degrees (see Figure 2). The intergranular aspect of the corrosion processes on these alloys is much more highly developed on Inconel 671 than on Inconel 690.

Corrosion rates for the high Ni-Cr alloys in solution B at 333K (not shown in Figure 1) were generally <0.004 mm/yr (0.16 mpy). The stainless steels (304L, 309S, 330SS and 347) exhibited delayed passivation. They appear to corrode at rates in the range of 10 to 100 mm/yr in the first hour and then quickly slow down to about 0.01 mm/yr after 100 h. After a few hundred more hours, the stainless steels exhibited corrosion rates similar to those observed for the high Ni-Cr alloys. It was also discovered that removing the stainless steel coupons from solution B for interim weighings resulted in passivation. This phenomenon is still under investigation and does not alter the overall result stated above.

The phenomenon of delayed passivation of the austenitic stainless steels is illustrated by the data plotted in Figure 3. The log (weight loss per cm^2 during the first 50 h or less of test) is plotted as a function of the Cr+Mo content for both stainless steels and some of the high Ni-Cr alloys for comparison. During this initial period, the corrosion rates of the stainless steels are three or more orders of magnitude greater than those observed for the high Ni-Cr alloys. As indicated above, after this initial high corrosion period, the corrosion rate for the stainless steels drops to a corrosion rate comparable to that of the high Ni-Cr alloys.

B. Surface Scale and Films

Two kinds of surface deposits formed during these tests. One was a green scale that formed particularly on coupons in solution A. In certain cases, this scale adhered tightly to the test coupon. The other kind of surface deposit was a submicron-thick film present on apparently clean metallic surfaces that could only be characterized by

TABLE 3. Certified Analyses of Metal Coupons (wt%)

Alloy	Cr	Ni + Mn + Co	Fe	Mo + Cu + W	Nb + Ta + Ti + Si	C	S	P
304L	18	9.9	71	0.0	0.48	0.01	0.011	0.031
347	18	12	69	0.15	1.35	0.05	0.003	0.029
309S	22	17	60	0.25	0.56	0.03	0.001	0.022
F-255[1]	26	5.9	62	5.30	0.70	0.02	0.006	0.018
904L[2]	20	26	46	5.81	0.40	0.01	0.003	0.018
Hayn. M. 20[3]	22	27	45	4.95	0.76	<0.01	0.012	0.017
330	20	37	42	0.04	1.18	0.01	0.005	0.017
Carp. 20Cb3[4]	20	34	40	5.28	0.84	0.024	0.001	0.015
Inc. 825[5]	23	43	28	4.56	1.48	0.01	0.001	-
Hast. G-30[6]	29	45	15	9.70	1.24	0.01	<.002	0.009
Hast. C-276	16	58	6.3	19.40	-	0.003	<.002	0.011
Hast. C-22	22	57	4.3	16.70	-	0.004	<.002	0.009
Hast. B	0.7	66	5.4	28.50	0.05	-	0.002	0.003
Inc. 617[7]	23	66	0.8	9.45	0.27 Al-1.2	0.06	0.001	-
Hast. C-4	15	69	0.6	14.90	0.22	0.003	<.002	<0.005
Inc. 625	22	64	1.6	8.90	3.66	0.025	0.005	0.005
Inc. 690	29	61	9.0	-	0.54	0.01	0.001	-
Inc. 671	46	54	0.1	-	0.39	0.05	0.003	-

[1]Ferrahum (255) is trademarked by Langley Alloys Limited, Buckinghamshire, England.
[2]Cabot (904L) is trademarked by Cabot Corporation, Kokomo, Indiana.
[3]Haynes (20 Mod.) is a trademark of Haynes International, Kokomo, Indiana.
[4]Carpenter (Carp. 20 Cb3) is trademarked by Carpenter Technology Corporation, Redding, Pennsylvania.
[5]Incoloy (Inc. 825) is a trademark of International Nickel Company, New York, New York.
[6]Hastelloy (Hast.) is a trademark of Haynes International Company, Kokomo, Indiana.
[7]Inconel (Inc. 617) is a trademark of the International Nickel Company, New York, New York.

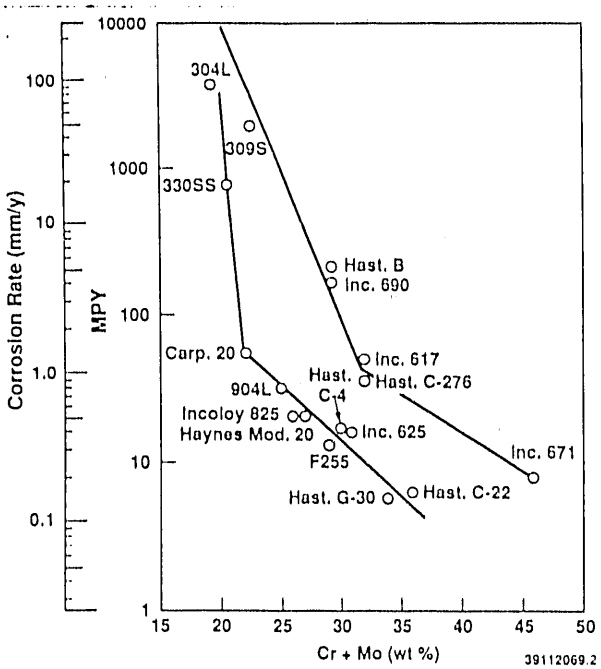

FIGURE 1. Observed Corrosion Rate in Solution A at 333K. The values plotted are taken from Table 4.

analytical instruments, such as Auger-Ion Milling and x-ray photoelectron spectroscopy (XPS).

The green corrosion scales, which adhered tightly to some of the coupons (i.e., the Inconels 617, 690, and 671) and loosely to others, were analyzed by x-ray diffraction and energy dispersion of x-rays (using a scanning electron microscope). These analyses indicated that the green scales were predominantly a sodium metal fluoride (Na_3MeF_6), where Me = Cr, Fe, Mo, and Ni. Typically, either Cr or Fe dominated the composition depending on the composition of the alloy on which the scale formed.

It is well known that stainless steels and high Ni-Cr alloys tend to passivate in oxidizing environments by forming an oxide film that greatly reduces the corrosion current and hence the corrosion reaction.[9] Because of the difference in corrosion results observed between the stainless steels and the high Ni-Cr alloys, and their reactions to solutions A and B, it was thought that there might be correlating differences in the oxide films present on their surfaces. Therefore, four pairs of coupons were chosen for surface evaluation to determine if clearly defined differences were present. The four pairs consisted of two each of the following alloys: Cabot 904L, Inconel 625, Hastelloy C-22, and 304L. One coupon each of three of the pairs of these high Ni-Cr alloy coupons was exposed to solution A and the other to solution B. The pair of 304L coupons were both exposed to solution B and observed to be passivated when they had been returned to solution B after an interim weighing. Coupon 304L-80 was weighed after 1 min in solution B and had a total exposure of 18 min, and coupon 304L-79 was weighed after 90 min in solution B and had a total exposure

TABLE 4. Corrosion Rates of "New Plant Alloys" in Solution A at 333K - Rationale for Values Chosen and Other Observations

Alloy	Test Time (h)	Rate (mpy) mm/y	Comments
304L	25	(3699) 94	Test discontinued after 25 h.
309S	25	(1880) 48	Test discontinued after 25 h.
F-255	66	(12.9) 0.33	Rate observed before the formation of an adherent corrosion scale.
904L	1945	(30.9) 0.78	
Haynes M. 20	985	(20.1) 0.51	Heavy, unevenly distributed pitting.
330SS	66	(753) 19	Test discontinued at 66 h.
Carp. 20	798	(55.5) 1.4	Patches of scale present on sample - not believed to cause a significant deviation in rate.
Inc. 825	774	(19.9) 0.51	See comment for Carpenter 20.
Hast. G-30	798	(5.7) 0.14	Some grain boundary attack.
Hast. C-276	1945	(34.6) 0.88	
Hast. C-22	798	(6.1) 0.15	Very light grain boundary attack.
Hast. B	704	(205) 5.2	
Inc. 617	66	(49.0) 1.2	Measurement made before the development of an adherent corrosion scale.
Hast. C-4	774	(16.7) 0.42	
Inc. 625	985	(15.6) 0.40	Patches of scale present on sample, not believed to cause a significant deviation in rate.
Inc. 690	40	(160) 4.1	Measurement made before the development of an adherent corrosion scale.
Inc. 671	66	(7.8) 0.20	Measurement made before the development of an adherent corrosion scale.

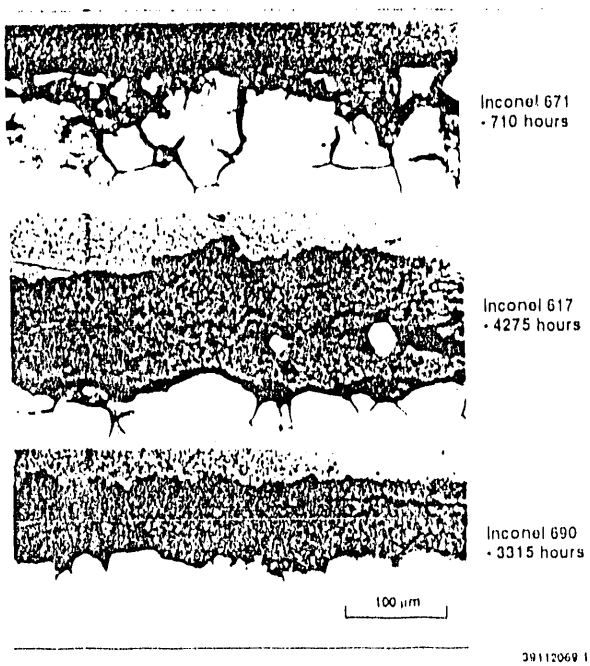

FIGURE 2. Photomicrographs of Polished Sections of Test Coupons of Inconel 671, 617, and 690 Exposed to Solution A at 333K Showing Varying Degrees of Intergranular Corrosion. In each micrograph the metal is at the bottom of the picture. The dark gray phase is the adhering corrosion scale. The hours indicate the duration of the test exposure.

of 105 min. Coupon 304L-79 was anticipated to be much closer to an equilibrium condition than coupon 304L-80.

These pairs were subjected to surface examination via Auger-Ion Milling (to determine the oxide film thickness) and XPS (to determine the oxide film composition). A tightly adherent corrosion scale (Na_3MeF_6) did not form onthese coupons possibly because of their smooth surface textures. The results of these evaluations are summarized in Tables 5 and 6.

Auger-Ion Milling determinations of the oxide film thickness are summarized in Table 5. The films formed in solution A are uniform and thin, barely a few atom layers thick. Films formed in solution B are on the order of 100 times thicker. In contrast, the oxide film formed on 304L in solution B is thin, similar to those formed by the high Ni-Cr alloys in solution A.

The surface compositions of the corrosion product films are given in Table 6. In addition to the elements included in the table, carbon (up to 30%) was also

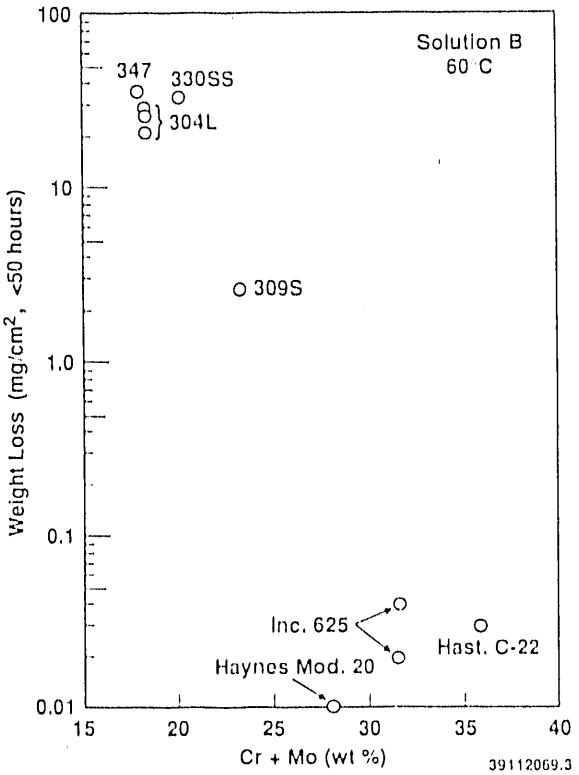

FIGURE 3. Short Term (<50 h on test) Coupon Weight Loss (per cm²) Illustrates the Effect of Delayed Passivation and Sensitivity to the Alloy Cr+Mo Content

TABLE 5. Oxide Film Thickness Determined by Auger-Ion Milling Depth Profile

Alloy	Solution A	Solution B
304L-79	-	90 Å
304L-80	-	108 Å
904L	35 Å	>5500 Å
Inc. 625	19 Å	2400 Å
Hast. C-22	14 Å	> 900 Å

indicated. However, carbon was not included in the tabulated analyses because adsorbed hydrocarbon from the atmosphere is a common surface contamination on specimens such as these, and the carbon present was ascribed to this source.

TABLE 6. Corrosion Product Film Composition Based on X-Ray XPS

Exposed to Solution A (atom%)

Alloy	O	Cr	Ni	Mo	F	Cu	Na	Zr	Si
904L	46.8	8.8	3.3	1.0	30.9	1.3	7.8	-	-
1625	37.2	10.0	6.8	2.7	27.3	-	16.0	-	-
C-22	52.5	13.0	8.5	4.0	19.6	-	2.2	-	-

Exposed to Solution B (atom%)

Alloy	O	Cr	Ni	Mo	F	Cu	Na	Zr	Si
304L-79	61.4	6.7	-	-	7.4	-	-	2.8	21.7
304L-80	65.8	2.5	-	-	2.7	-	-	2.1	26.8
904L	49.5	-	-	-	28.9	-	-	12.8	8.8
1625	50.4	-	-	-	28.2	-	-	12.6	8.7
C-22	43.3	-	-	-	36.8	-	-	15.4	4.5

There are distinct compositional differences in films that form in contact with the two solutions. In solution A, an oxide film forms that is enriched with chromium relative to the other alloy constituents. The fact that there is considerable fluorine and sodium on the surface suggests that oxyfluorides and sodium metal fluoride salts (the corrosion scale already described) are present also. In solution B, the film is entirely composed of elements already present in the solution (except for the chromium observed on the 304L surface), and sodium is conspicuous by its absence.

V. DISCUSSION AND INITIAL CONCLUSIONS

In relatively simple acid solutions with high HF activity (such as solution A), high Ni-Cr alloys with >5% Mo display useful corrosion resistance. The stainless steels tested do not. When the HF activity is lowered through the addition of complexing elements (viz., zirconium and silicon in solution B), the corrosion rate drops, but for more reasons than the reduction of HF activity. The stainless steels tested show delayed passivation with a final rate similar to that observed for the high Ni-Cr alloys. However, the passivating film on the 304L stainless is distinctly different (Tables 5 and 6) than that observed on the high Ni-Cr alloys in solution B. The passivating film on the high Ni-Cr alloys is considerably thicker than that on the 304L and could be more resistant to erosion by solution B.

The critical difference between the high Ni-Cr alloys and the stainless steels with respect to their behavior in solution A appears to be their Cr+Mo content (Figure 1). The enrichment of the metal surface in chromium is known to occur as 304 and iron based Cr+Mo alloys passivate. It is also known that molybdenum accelerates and may accentuate the surface chromium enrichment.[10] The XPS surface analyses given in Table 6 show a progressively higher chromium content in the surface film for the three alloys, which also correlates with a progressively lower corrosion rate. (A similar measurement on stainless steel samples exposed to solution A has not been taken.) The oxide film observed on the high Ni-Cr alloys (Table 5) exposed to solution A is similar in thickness to the passivating film that develops on iron and iron based alloys[11] and appears to be typical of such films. Regarding the amount of Cr+Mo, test results appear consistent with effects observed in similar alloy systems. The increase in the Cr+Mo to above 20% to 25% is necessary for the development of effective passivating films in acid environments.

The sodium metal fluoride salt film essentially encased some of the specimens making it impossible to get long term corrosion results on some of the alloys by the determination of weight change, (i.e., Inconel 671, 617, and 690). It appeared to be the intergranular corrosion of these alloys that allowed the scale to become firmly anchored to the coupon surface, physically passivating the specimen. The sodium and some of the fluoride observed in the surface films (Table 6) are likely due to the presence of the Na_3MeF_6 compound previously described. Fluoride could also be present in the film replacing hydroxide in the oxide film since hydroxides are believed to be present in films formed in other aqueous corrosion environments. The formation of the salt scale occurs when any of the alloys tested are exposed to solution A and will need to be considered in any chemical processing system built to handle a solution similar to solution A.

The stainless steels and the high Ni-Cr alloys corrode at similar rates in solution B at 333K, though they take differing amounts of time to attain similar rates and display a distinctly different passivating film after that time. As described in the previous section, the stainless steels display delayed passivation in solution B, i.e., they show a large initial corrosion rate that decreases by several orders of magnitude after a brief time period (on the order of an hour) and finally approach the low corrosion rates (displayed by the high Ni-Cr alloys from the beginning) after approximately 100 h. When the thickness of the passivation films are measured, one sees not only a significant difference in thickness, but a difference in composition as well. The 304L (representing the stainless steels) has a relatively thin film when compared with the high Ni-Cr alloys, and it is not known whether the small difference in thickness or composition between coupons is significant. The high Ni-Cr alloys, on the other hand, display distinctly thicker films that do not appear to contain any components originating from the metal substrate. Their compositions appear to be almost identical. It appears that components (i.e., silicates) from the solution may behave like inhibitors by attaching themselves to the surface to block the corrosion reaction.

There are probably at least three or four factors, not including alloy composition and textural properties, that are controlling the corrosion rates in these tests. One factor is the oxidation potential of the solution. For these tests, the oxidation potential will be determined by the nitric acid concentration and the degree of solution aeration, which will tend to passivate the alloys by developing protective oxide films. The HF activity is expected to be a depassivating factor, removing metals from the passivating film by forming fluoride salts. The scale that forms can also passivate a surface if it is dense enough, as observed with several of the Inconels. Also, there are the inhibition effects of other solution components, such as silicate, which seem to have deposited from solution B. Hence, it should not be expected that change in HF activity alone controls the corrosion behavior of the high Ni-Cr alloys in acid fluoride wastes, but a combination of interrelated factors that are not yet understood.

Future studies that will include corrosion of weldments, erosion corrosion, stress corrosion, and localized corrosion. Erosion corrosion is a potentially important phenomenon because these alloys are passivated by a film of unknown durability. The investigation of weldment corrosion is expected to reveal any problems associated with sensitization. Also, stress corrosion cracking is always a question when a material forms a passive film.

Overall, the high Ni-Cr alloys are the materials of choice for new plant construction. Presently, Hastelloys C-22 and G-30 are the leading candidates because of their superior performance in solution A at 333K. If the TRUEX chemical processing solutions projected for use have an HF activity less than that of solution B, some stainless steels may be suitable. However, the delayed passivation displayed by the stainless steels in solution B suggests that they be considered with caution until more positive corrosion resistance is observed.

VI REFERENCES

1. S. A. BARKER, E. B. SCHWENK, and J. R. DIVINE, "Materials Evaluation for a Transuranic Processing Facility," WHC-SA-0963-FP, Westinghouse Hanford Company, Richland, Washington, (presented American Nuclear Soc., 1990 Winter Meeting, Washington, D.C., November 11-15, 1990) (1990).

2. ASM International, "Corrosion," Metals Handbook, 9th edition, 13, 650 (1987).

3. R. S. ONDREJCIN, and B. D. MCLAUGHLIN, "Corrosion of High Ni-Cr Alloys and Type 304L Stainless Steel in HNO_3-HF," DP-1550, Savannah River Laboratory, E. I. DuPont de Nemours and Company, Aiken, South Carolina (1980).

4. R. F. MANESS, "Corrosion of 304-L Stainless Steel and HAPO-20 in Acid-Fluoride Systems," HW-80658, Hanford Laboratories, General Electric Company, Richland, Washington (1964).

5. R. F. MANESS, "Power Reactors Fuels Reprocessing Progress Report on Corrosion Studies," HW-61662, Hanford Atomic Products Operation, General Electric Company, Richland, Washington (1959).

6. B. J. NEWBY, and T. L. HOFFMAN, "Blending Raffinates from Zirconium and Aluminum Processes," IN-1114, Idaho Nuclear Corporation (1967).

7. H. S. COLE, "Corrosion of Austenitic Stainless Steel Alloys Due to HNO_3 - HF Mixtures," ICP-1036, Allied Chemical Corporation, Idaho Chemical Programs Office (1974).

8. R. R. HAMMER, "A Determination of the Stability Constants of a Number of Metal Fluoride Complexes and Their Rates of Formation," ENICO-1004, prepared for the Department of Energy, Idaho Operations Office (1979).

9. NACE, "Passivity and Its Breakdown on Iron and Iron Based Alloys," R. W. Staehle, and H. Okada, editors, U.S.A.-Japan Seminar, March 10-12, 1975, (1976).

10. Ibid, pages 82-84, H. Okada, H. Ogawa, I. Itoh, and H. Omata, "Auger Electron Spectroscopic Analysis of the Passive Film of Stainless Steels."

11. Ibid., discussion, pages 85-87, "Nature of the Passive Film on Iron and Iron Based Alloys."

END

DATE
FILMED
6/23/92